Molecular Targets for Diabetes Mellitus-associated Erectile Dysfunction*

Elizabeth Yohannes‡, Jinsook Chang‡, Moses T. Tar§, Kelvin P. Davies§, and Mark R. Chance‡¶‖

Protein expression profiles in rat corporal smooth muscle tissue were compared between animal models of streptozotocin-induced diabetes mellitus (STZ-DM) and age-matched controls (AMCs) at 1 week and 2 months after induction of hyperglycemia with STZ treatment. At each time point, protein samples from four STZ-DM and four AMC rat corpora tissues were prepared independently and analyzed together across multiple quantitative two-dimensional gels using a pooled internal standard sample to quantify expression changes with statistical confidence. A total of 170 spots were differential expressed among the four experimental groups. A subsequent mass spectrometry analysis of the 170 spots identified a total of 57 unique proteins. Network analysis of these proteins using MetaCore™ suggested altered activity of transcriptional factors that are of too low abundance to be detected by the two-dimensional gel method. The proteins that were down-regulated with diabetes include isoforms of collagen that are precursors to fibril-forming collagen type 1; Hsp47, which assists and mediates the proper folding of procollagen; and several proteins whose abundance is controlled by sex hormones (*e.g.* CRP1 and A2U). On the other hand, proteins seen or predicted to be up-regulated include proteins involved in cell apoptosis (*e.g.* p53, 14-3-3-γ, Serpinf1, Cct4, Cct5, and Sepina3n), proteins that neutralize the biological activity of nerve growth factor (*e.g.* anti-NGF 30), and proteins involved in lipid metabolism (*e.g.* apoA-I and apoA-IV). Subsequent Western blot validation analysis of p53, 14-3-3-γ, and Hsp47 confirmed increased p53 and 14-3-3-γ and decreased Hsp47 levels in separate samples. According to the results from the Western blot analysis, Hsp47 protein showed a ~3-fold decrease at 1 week and was virtually undetectable at 2 months in diabetic *versus* control. Taken together, our results identify novel candidate proteins playing a role in erectile dysfunction in diabetes resulting from STZ treatment. ***Molecular & Cellular Proteomics 9:565–578, 2010.***

Erectile dysfunction (ED)[1] is one of the many complications caused by diabetes mellitus. About 52% of men between the age of 40 and 70 years suffer from ED due to various causes, such as pathophysiological changes in nerves, blood vesicles, corporal smooth muscle tissue, and endothelial cells as well as psychological problems (such as stress) (1–3). As most of these risk factors for development of ED are inherent to diabetes mellitus, men with diabetes have a greater prevalence of ED and early onset of the disease compared with men without diabetes (4–6). The current estimates suggest that as many as 75% of men with diabetes will develop some degree of ED at an earlier age (7). In addition, men with diabetes present with more severe dysfunction and are less responsive to current pharmacological therapies for ED (8–10). Although ED is considered a disease impacting the "quality of life" of patients, it is often associated with depression, low self-esteem, and lower overall quality of marital relations. The pathogenesis of ED in diabetes mellitus at the molecular level remains poorly understood.

The most common predictors of erectile dysfunction in patients or model animals with diabetes are hypogonadism (11–13), neuropathy (14, 15), arterial insufficiency (16, 17), progressive loss of both the endothelium and smooth muscle tissue (1), and impaired regulation of smooth muscle tone (18). Diabetes decreases the testosterone levels (androgen) in patients and in the streptozotocin (STZ)-induced diabetic rat model (19–21). Androgen deficiency in rats is associated with down-regulation of the neuronal isoforms of nitric-oxide synthase (14, 20). In addition, fluctuating blood sugar levels can modulate nitric oxide synthesis in endothelial cells (22, 23), cause increased accumulation of advanced glycation end products (24, 25), and up-regulate arginase, a competitor with nitric-oxide synthase for its substrate, L-arginine (26). Nitric oxide (NO)-mediated neurotransmission is impaired in smooth muscle relaxation and decreases arterial inflow in the penile circulation and corpora cavernosa (27, 28). Relaxation re-

From the ‡Center for Proteomics and Bioinformatics and ¶Department of Physiology and Biophysics, Case Western Reserve University, Cleveland, Ohio 44106 and §Department of Urology, Albert Einstein College of Medicine, Bronx, New York 10461

Received, June 23, 2009, and in revised form, October 21, 2009
Published, MCP Papers in Press, December 10, 2009, DOI 10.1074/mcp.M900286-MCP200

[1] The abbreviations used are: ED, erectile dysfunction; DM, diabetes mellitus; AMC, age-matched controls; STZ, streptozotocin; NGF, nerve growth factor; 2D, two-dimensional; BVA, biological variation analysis; DIA, differential in-gel analysis; ANOVA, analysis of variance; PCA, principal component analysis; O-TOF, orthogonal TOF; ICP, intracorporal pressure; BP, systemic blood pressure; HDAC1, histone deacetylase 1; Hsp47, heat shock protein 47; CRP, cystatin-related protein; A2U, α-2u-globulin; PEDF, pigment epithelium-derived factor; 2,3-BPG, 2,3-bisphosphoglycerate; MPZ, myelin protein zero.

sponses of the smooth muscle could also be altered through changes in the Ca^{2+} sensitization pathways (18). Blood vessels can also become narrowed or hardened (atherosclerosis) by conditions that often accompany diabetes, such as cardiovascular disease (29–31). When atherosclerosis occurs in arteries that supply blood in the penis or pelvic area, sexual function may be disrupted. Thus, it is clear that diabetes has the potential to impact all components of the erectile response.

There have been major advances in the identification of genes and signaling pathways involved in erectile dysfunction (17, 32–34); however, to our knowledge, there are no studies that have been conducted to characterize the protein changes at the proteome level. As there is a modest correlation between transcription and protein expression levels, there are obvious opportunities to advance our molecular understanding of the disease by direct measurements of protein changes. Moreover, diabetes-associated ED has progressive features, yet there are no reports of systematic -omic level studies that have focused on the initiation, development, and progression of the ED in diabetic patients or model animals. The present study was undertaken as a first step to elucidate the effect of diabetes at the protein level in corporal tissue, thereby providing a more integrative understanding of erectile physiology and/or dysfunction. Differential protein analysis was carried out using two-dimensional (2D) DIGE coupled with mass spectrometry to compare and identify proteins that are changing at 1 week and at 2 months after the induction of hyperglycemia in an STZ-DM rat model compared with age-matched controls. Although animal models, in general, may recapitulate only some aspects of human disease, this model system is of particular interest to our studies as it appears to mimic many relevant aspects of human ED (32, 35, 36). Another advantage of the animal model is that it is also possible to examine potential proteome profile shifts in the erectile tissue at selected time points, even prior to any overt presentation of clinical symptoms in the disease progression.

Our experimental design included four experimental groups (1-week STZ-induced diabetic, 1-week age-matched control, 2-month STZ-induced diabetic, and 2-month age-matched control). For each experimental group, four independent biological replicate samples were prepared and analyzed across multiple 2D DIGE gels using a pooled internal standard sample that ensured precise quantification of expression changes and their detailed statistical analysis (37–42). Also, quantitative measurements of the intracorporal pressure/systemic blood pressure ratio following electrical stimulation of the cavernous nerve were made to confirm the functional deficits of the treated rats.

Although this study design and the attendant statistical analysis provide precise and accurate readouts of protein abundance changes, a potential disadvantage of the method is that it fails to capture a substantial fraction of the total proteome. Thus, although proteomics methods may not have broad coverage of the proteome (42–44), the targets we identified are important members of cellular pathways involved in a wide range of biological processes and functionally relevant to the disease. To leverage the protein abundance changes, they were used as inputs for bioinformatics analysis of pathways possibly involved in the disease process (43–46). Thus, we analyzed the targets provided by the 2D DIGE experiments using MetaCore™ pathway analysis tools (47, 48). These analyses provided additional molecular targets of interest in the disease, and some of these hypothesized targets along with some targets detected directly by 2D DIGE were examined by Western blotting. With this integrated approach, we identified a number of differentially expressed proteins that could provide valuable mechanistic insight into the molecular changes that are precursors for and/or associated with DM-induced ED.

MATERIALS AND METHODS

The majority of chemicals in this study were obtained from GE Healthcare (formerly Amersham Biosciences), Thermo Fisher Scientific (formerly Pierce), and Invitrogen and used without further purification unless otherwise stated. Mouse monoclonal anti-heat shock protein 47 (Hsp47), anti-14-3-3-γ, anti-MPZ, anti-histone deacetylase 1 (HDAC1), anti-β-actin, loading control (Abcam), and anti-p53 (Santa Cruz Biotechnology) antibodies specific for human, rat, and mouse were purchased from the indicated vendors.

Animal Preparation—Diabetes was induced in male Fischer 344 rat (Taconic Farms, Germantown, NY; 8–10 weeks old and weighing 200–240 g) with a single intraperitoneal injection of STZ (35 mg/kg) dissolved in citrate buffer (0.6 M citric acid, 0.08 M Na_2HPO_4, pH 4.6) as described previously (33, 42, 49). The age-matched control (AMC) rats received an injection of vehicle only. All procedures were approved by the Animal Institute Care and Use Committee at Albert Einstein College of Medicine. Initiation of the diabetic state was confirmed by the presence of high blood glucose levels for the STZ-treated animals, and maintenance of diabetes was reconfirmed at animal sacrifice (control, 132 $\pm$ 14 mg/dl glucose; STZ-treated rats at 1 week, 537 $\pm$ 22 mg/dl; and STZ-treated rats at 2 months, 562 $\pm$ 18 mg/dl).

Measurement of Intracorporal Pressure/Systemic Blood Pressure (ICP/BP)—One week or 2 months following confirmation of STZ-induced diabetes, the rats were anesthetized with pentobarbital sodium (35 mg/kg intraperitoneally), and erectile function was determined by measuring the ICP/BP ratio following electrical stimulation of the cavernous nerve as described previously (33, 49). Briefly, an incision was made in the perineum, and a window was made in the ischiocavernosus muscle to expose the corpus cavernosum. The cavernous nerves were identified adjacent to the prostate gland. The cavernous nerve was directly electrostimulated with a delicate stainless steel bipolar hook electrode attached to a multijointed clamp. Each probe was 0.2 mm in diameter, and the two poles were separated by 1 mm. Monophasic rectangular pulses were delivered by a signal generator that was custom-made with a built-in constant current amplifier. Stimulation parameters were as follows: frequency, 20 Hz; pulse width, 0.22 ms; duration, 1 min; and current, 0.75 and 4 mA. Changes in ICP and BP were recorded at each intensity of stimulation. In each group, a minimum of five animals were used to determine ICP/BP. Significant differences between treatment groups were determined by Student's *t* test. Once the ICP/BP was measured, the animals were sacrificed. The corpus cavernosum, consisting predom-

TABLE I
Experimental design for 2D DIGE proteome profiling

Four biological replicate samples for each group (C_1W, control sacrificed at 1 week after vehicle injection; D_1W, 1 week after the confirmation of STZ-induced diabetes; C_2M, 2 months after vehicle injection; and D_2M, 2 months after the confirmation of STZ-induced diabetes) were used and labeled with Cy3 or Cy5. Each gel contained the pooled standard (mixture of equal aliquots of each sample in all experimental groups) and two other subject samples. Thus, the 16 samples were analyzed in triplicate by running eight gels. (For detailed descriptions, refer to "Materials and Methods.")

Gel	Cy3	Cy5	Cy2
1	C1_1W	D1_1W	Pooled internal standard sample (C1–4_1W + D1–4_1W + C1–4_2 M + D1–4_2M)
2	D2_1W	C2_1W	Pooled internal standard sample (C1–4_1W + D1–4_1W + C1–4_2 M + D1–4_2M)
3	C3_1w	D3_1W	Pooled internal standard sample (C1–4_1W + D1–4_1W + C1–4_2 M + D1–4_2M)
4	D4_1W	C4_1W	Pooled internal standard sample (C1–4_1W + D1–4_1W + C1–4_2 M + D1–4_2M)
5	C1_2M	D1_2M	Pooled internal standard sample (C1–4_1W + D1–4_1W + C1–4_2 M + D1–4_2M)
6	D2_2M	C2_2M	Pooled internal standard sample (C1–4_1W + D1–4_1W + C1–4_2 M + D1–4_2M)
7	C3_2M	D3_2M	Pooled internal standard sample (C1–4_1W + D1–4_1W + C1–4_2 M + D1–4_2M)
8	D4_2M	C4_2M	Pooled internal standard sample (C1–4_1W + D1–4_1W + C1–4_2 M + D1–4_2M)

inantly of smooth muscle tissue, was excised from each animal, flash frozen in liquid nitrogen, and stored at −80 °C until used for the downstream protein analyses.

Protein Extraction and Fluorescent Dye Labeling—The experiments were designed to monitor changes in protein abundance as a function of disease progression, to generate statistically significant results, and to minimize in-gel and gel-to-gel systematic variations. Thus, the corpora tissue samples examined consisted of AMC Fisher 344 rats sacrificed 1 week ($n = 4$) and 2 months ($n = 4$) following vehicle injection and STZ-induced diabetic Fisher 344 rats sacrificed 1 week ($n = 4$) and 2 months ($n = 4$) following STZ-induced diabetes. Overall, this study design was expected to provide a power of 0.8 to detect 50% or greater change in protein expression in at least 75% of the detected spot entities using the DIGE method (see "Results" below).

Sample preparation was conducted as described previously (42). Briefly, the frozen tissue samples were disrupted by grinding in liquid nitrogen with a mortar and pestle. The tissue powder was then homogenized in lysis buffer (7 M urea, 2 M thiourea, 4% (w/v) CHAPS, 30 mM Tris) with five cycles of freeze, thaw, and sonication. After the supernatant was collected and cleaned, the concentration was determined, and the supernatant was further diluted with lysis buffer to give stock solutions with final protein concentrations of 5 mg/ml. Sixteen aliquots, each with 25 μg of protein, were collected from the control and STZ-induced diabetic samples and pooled to prepare internal standard samples. Thus, samples from either control or STZ-induced diabetic corpora tissue were labeled with Cy3 or Cy5 cyanine dyes and the internal standard sample was labeled with Cy2 dye by the addition of 400 pmol of CyDye in 1 μl of anhydrous *N*,*N*-dimethylformamide/50 μg of protein. A dye-swapping scheme, as shown in Table I, was used such that the four samples for any condition were variously labeled with Cy3 or Cy5 to control for any dye-specific labeling artifacts. Labeling was performed for 30 min on ice in the dark; the reaction was then quenched with 10 mM lysine and additionally incubated for 10 min.

Gel Electrophoresis—The quenched Cy3- and Cy5-labeled samples, to be partitioned in the same gel according to the experimental design in Table I, were then combined and mixed with an aliquot of Cy2-labeled standard and an equal volume of 2× sample buffer (8 M urea, 4% (w/v) CHAPS, 2% (w/v) DTT, 2% (v/v) Pharmalytes pH 3–10 non-linear) was added. Prior to IEF, an additional 350 μg of unlabeled protein was added (for later spot picking), and the mixtures were brought up to 450 μl with 1× rehydration buffer. The mixed samples were then partitioned according to their pI and then molecular weight in two-dimensional gels as described previously (42).

Image Acquisition and Spot Quantification—Gel image acquisition and spot quantification were carried out as described previously (42). Briefly, data analysis was carried out using a total of 24 gel images consisting of four biological replicate images from 1-week control, four replicates from 1-week treated, four replicates from 2-month control, four from the 2-month treated, and eight from the internal standards, which were pooled mixtures of equal aliquots of each experimental sample. The pick gel image was also processed with the rest of the gel images as a pick gel image but not included in the analysis. To compare protein spots across the eight gels, image analyses were conducted into two steps using DeCyder v6.5 2D differential analysis software (GE Healthcare). In the first step, the set of three images from a single gel were loaded into the differential in-gel analysis (DIA) algorithm within the DeCyder software. Intragel spot detection and quantification were performed using the DeCyder 2D software DIA module. For the subsequent intergel differential analysis, the DIA work spaces for all the gels were saved and loaded into the biological variation analysis (BVA) module. In the BVA module, the image with the largest number of protein spots was assigned as the master image. Sample (Cy3- or Cy5-labeled) spot maps were assigned into four groups (group 1, AMC 1 week; group 2, STZ-induced diabetic 1 week; group 3, AMC 2 months; and group 4, STZ-induced diabetic 2 months), and all internal standard and pick spot maps were assigned into standard and pick folders, respectively, in the experimental design view of the BVA modules. Once the spots from the common standards were matched across the eight gel images and with the pick gel image, the standardized volume ratio for each standard image from the different gels was set to the value 1.0 to compare ratios between matched protein spots in the different gels (groups). Thus, the ratios of the log-standardized protein spot abundances (differences in expression) between the groups were computed.

To test for significant differences in expression of proteins between the experimental groups, one-way analysis of variance (ANOVA) was performed at a significance level of 0.05; thus, for every 100 spots tested, five false positives would be expected. In addition, two-way ANOVA treatment, two-way ANOVA time, and two-way ANOVA interaction were computed to assign statistically significant changes in spot intensity due to the treatment alone, time alone, and both treatment and time. The data were filtered using the average volume ratios of 1.5 and above or −1.5 and below -fold differences in expression and with a one-way ANOVA p value of 0.05 or less and assigned to a spot of interest. For the spots that displayed significant differences in expression among the groups, a pick list with pick location and coordinates was generated. The pick list along with the poststained pick gel was transferred to the automated Ettan spot picker, and excised gel plugs were placed into a 96-well plate for the subsequent in-gel digestion and mass spectrometry analysis of the peptide for protein identification.

Multivariate analyses were performed on the expression data derived from the BVA using the DeCyder extended data analysis software. The gel images were grouped such that the four biological replicates for each experimental condition formed a group. This resulted in four groups each representing the experimental condition. Once the BVA was imported into the extended data analysis software, the data were filtered so that only 170 spot features exhibiting statistically significant (ANOVA $p < 0.05$) changes and present in more than 80% of the spot maps were considered. The global relationships among spot maps were visualized by performing a principal component analysis (PCA) on these spot features.

In-gel Digestion and Protein Identification—The proteins in the gel plugs were digested with trypsin (Promega) using a modified protocol adapted from Shevchenko *et al.* (50). Tryptic digests were extracted from the gel matrix and concentrated by SpeedVac, avoiding complete drying. For mass spectrometric analysis using MALDI, aliquots of the concentrated peptides were treated and eluted off of the ZipTip (Millipore, Billerica, MA) according to the instruction manual and directly deposited onto a MALDI target plate with a matrix solution (at a concentration of 5 mg/ml in 50% ACN, 0.1% TFA). Mass spectra were acquired on a prOTOF 2000™ MALDI O-TOF mass spectrometer (PerkinElmer Life Sciences) in the positive ion mode using TOFworks™, an integrated work flow-based software platform. The peptide ion masses (M + H) were accurate to within 10 ppm after external calibration using an external calibration mixture, pepmix 1, ProXpression MALDI standard kit (PerkinElmer Life Sciences). Monoisotopic peptides peak lists were generated in the mass range *m/z* 500–5000 with a signal to noise ratio threshold of 3.0 and peak resolution threshold of 10,000 using the M/z peak picking algorithm (Genomic Solutions, Ann Arbor, MI) of the TOFworks software version 1.0.1.798. Trypsin autolysis fragment peaks and peaks from the matrix were not excluded unless otherwise stated. The resulting peptide mass lists were used to search the sequences present in an indexed rat subset database (36,274 sequences), created from the National Center for Biotechnology Information non-redundant (NCBInr) database (3,893,302 sequences; release July 4, 2006) and stored locally, by running ProFound™ search engine version 2003.6.2.1 (Genomic Solutions). Search parameters used in this study were: 1) protein molecular mass search window, 10–300 kDa; 2) protein expectation, $p < 0.001$; 3) minimum sequence coverage, 10%; 4) peptide mass tolerance limits, 30 ppm; and 5) complete cysteine modification by iodoacetamide (57 Da), partial methionine oxidation (16 Da), and two missed cleavage sites allowed. A positive identification was accepted when a minimum of six peptide monoisotopic masses matched a particular protein with a mass error tolerance of ≤30 ppm, sequence coverage ≥10%, and low expectation value ($p < 0.001$) (all the data are presented in supplemental Table 2 and supplemental Fig. 1, a–g).

In cases where peptide mass fingerprinting did not result in positive identification, we performed LC-MS/MS experiments. Thus, tandem mass spectra for the rest of the gel plugs were acquired using a Fourier transform LTQ mass spectrometer (Thermo Electron Corp., Bremen, Germany). Separation of peptides via capillary liquid chromatography was performed using a Dionex Ultimate 3000 capillary LC system. Mobile phase A (aqueous) contained 0.1% formic acid in 5% acetonitrile, and mobile phase B (organic) contained 0.1% formic acid in 85% acetonitrile. The protein digests were trapped onto a precolumn (C_{18}, PepMap100, 300 μm × 5 mm, 5-μm particle size, 100 Å, Dionex) and desalted on line in mobile phase A at 10 μl/min for 10 min. The sample was subsequently loaded onto a Dionex C_{18} PepMap 75-μm × 15-cm reversed phase column with 5% mobile phase B. Separation was obtained with a linear gradient of 2%/min, starting with 100% mobile phase A. Subsequently, the peptides were infused at a flow rate of 300 nl/min via a PicoTip emitter (New Objective Inc., Woburn, MA) and at a voltage of 1.8 kV. Mass spectrum data were acquired using alternating full MS scan and MS/MS scans. Survey data were acquired from *m/z* 400–1600, and the precursors were interrogated by MS/MS per switch. The switch into MS/MS was based on precursor intensity, and three scans were acquired for every precursor interrogated. The tandem mass spectra were annotated, and peak list files were generated, commonly referred to as .DTA files, by running SEQUEST extract_msn algorithm in Bioworks version 3.2 (Thermo Electron Corp.). The mass range *m/z* 400–3500 from full scan data with an absolute threshold of 100, a minimum ion count of 12, and a precursor ion tolerance of 1.4 Da was used to generate the .DTA file. Prior to searching, non-redundant databases of 3,893,302 sequences (release July 4, 2006) were downloaded in FASTA format via file transfer protocol from the web site of the NCBInr. These databases were stored locally, and a subset of the database for rat species was created and indexed to produce faster search times. The resulting peak list (.DTA) files were then used to interrogate sequences present in an indexed rat subset database (36,274 sequences stored locally) by running the SEQUEST SEARCH algorithm of Bioworks software version 3.2. SEQUEST searches were performed with maximum peptide and fragment ion mass tolerances of 2.5 and 1.0 Da, respectively, with partial methionine oxidation, complete carbamidomethylation of cysteine, and two missed cleavage sites allowed in the search parameters. The criteria for each protein identification were as follows: a minimum of two peptides with a significant peptide expectation ($p < 0.001$); peptide Xcorr values of 1.9, 2.7, and 3.5 for the charge states 1+, 2+, and 3+, respectively; and a minimum ΔCN (delta correlation) of 0.1. In addition, all the MS/MS spectra identified by SEQUEST were manually verified for spectral quality and matching y and b ion series (all the data are presented in supplemental Table 3).

Network Analysis—The data set with a list of regulated proteins identified by 2D DIGE/MS was analyzed further by pathway analysis using the network building tool MetaCore (GeneGo, St. Joseph, MI). MetaCore consists of curated protein interaction networks on the basis of manually annotated and regularly updated databases. The databases consist of millions of relationships between proteins that are derived from literature publications on proteins and small molecules. The relationships include direct protein interaction, transcriptional regulation, binding, and enzyme-substrate and other structural or functional relationships. The networks can be visualized graphically as nodes (proteins) and edges (the relationship between proteins) alongside the empirical expression pattern. The data set from our study consisting of the proteins with statistically significant -fold changes identified by 2D DIGE/MS and gene name as a tab-delimited file was imported into MetaCore. Hypothetical networks of proteins from our experiment and proteins from the MetaCore database were then built using the shortest paths algorithm, one of the several algorithms integrated within MetaCore.

Immunoblotting Analysis—The corpora tissue lysates (10 μg of protein/lane) were prepared from two biological replicates of STZ-induced diabetic and age-matched control. Equal amounts of protein (10 μg/lane) were loaded and separated by electrophoresis on denatured and reduced 4–20% polyacrylamide gels (Invitrogen). The proteins were then transferred onto nitrocellulose membranes. The membranes were blocked with 5% skim milk for 1 h at room temperature with gentle shaking, washed, and incubated overnight with primary antibody at 1 μg/μl (at 1:2000 dilution). The membrane was washed and then incubated for 1 h at room temperature with the secondary antibody at 2 μg/μl (1:10,000 dilution) horseradish peroxidase-conjugated rabbit polyclonal anti-mouse IgG or horseradish peroxidase-conjugated goat anti-rabbit IgG. After three washing steps, the blot was incubated for 5 min in chemiluminescence-developing substrates prepared according to the manufacturer's instructions (Pierce). The membrane was removed from the substrates and

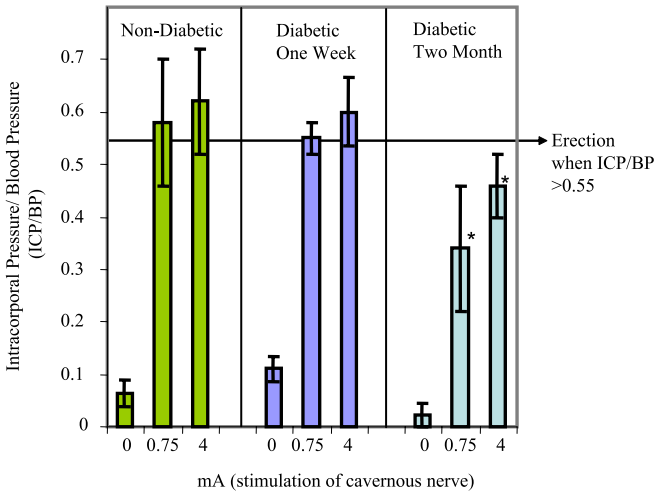

FIG. 1. **Decreased erectile function in diabetic animals in response to cavernous nerve stimulation.** The mean change in ICP/BP (*, $p < 0.05$ compared with non-diabetic) is shown. The error bars represent the standard deviation from the mean.

placed in plastic sheet protectors, and the chemiluminescence was visualized by exposure of the blot on Kodak X-Omat film. The blot was scanned, and the protein bands were quantified using ImageQuant-TL v2005 software (GE Healthcare). Equal loading of the protein samples was illustrated by reprobing the blots for β-actin (see Figs. 5 and 6).

RESULTS

Glucose Level—Blood glucose was significantly higher in diabetic rats relative to AMCs. In AMCs (1 week and 2 months), the average blood glucose levels were 132 ± 14 mg/dl, and in STZ-treated diabetic rats, the average blood glucose levels at 1 week were 537 ± 22 mg/dl and at 2 months were 562 ± 18 mg/dl. These levels were maintained throughout the course of the study.

ICP Responses to Nerve Stimulation—Electrical stimulation of the cavernous nerve resulted in a stimulus-dependent increase in ICP (Fig. 1). The ICP/BP ratio is useful in determining erectile function. The mean ICP/BP (from five biological replicates) was lower at all applied currents in the 2-month diabetic group compared with AMCs and 1-week diabetic animals (statistically significant at 0.75 and 4 mA, $p < 0.05$). All of the 2-month diabetic group animals failed to demonstrate a visible erection even at the highest level of stimulation. This confirmed the presence of diabetes-associated ED in the 2-month STZ-treated animals, and the observed reductions in ICP/BP are consistent with previously reported values of ICP responses in Fischer 344 diabetic rats (32, 35).

Protein Spot Quantification and Statistical Analysis—The experiment was designed to minimize both false-positive and false-negative results for expressed proteins while defining a minimal detectable difference (the smallest difference between the treatments that we wished to be able to detect). Four full replicates (with respect to model animal preparation, protein isolation, sample preparation, and 2D DIGE) were performed for each experimental condition. To estimate the number of samples providing enough power to detect differences in the protein level among experimental groups, sample size and power analysis was performed for several proteomics data sets that we already had in the center. The within-group median variances for the spots that are present in all gels, about 75% of the total spots detected in the gel, were calculated on the data sets from similar types of tissue used in this study. The power curves per hypothesis of the two-sided *t* test were then generated as a function of sample size required to detect 1.3-. 1.5-, 2-, and 4-fold changes of protein spots at the 0.05 level of significance (for details, see Ref 44). From the power curve, the minimum numbers of samples required to detect a particular -fold change were estimated. Thus, the sample size estimated to detect difference in means of 50% or more with 80% power was four per experimental group.

Thus, spots with 1.5 and above or −1.5 and below -fold changes and that exhibited statistically significance (one-way ANOVA p value <0.05) were retained in this study. Once the spots were detected to be significant, the spots were carefully checked for correct matching throughout all the gels. Of a total of 1180 spots that were matched in more than 80% of spot maps, the mean intensities of 170 spots were considered to be significantly different among the experimental groups and were further investigated as spots of interest. For these 170 spots whose overall expression profile yielded a significant one-way ANOVA p value, a Tukey procedure was used to determine for which two groups the ratio of the expression changes was significant; these are indicated in boldface in supplemental Table 1. In addition, to evaluate the statistical significance of effects either of STZ-induced diabetes or duration of diabetes on protein spot expression and also to determine whether there was an interaction effect between the STZ-induced diabetes and time, the data were further filtered by two-way ANOVA treatment, two-way ANOVA duration, and/or two-way ANOVA interaction ($p \leq 0.05$). Of the total 170 spots that were differentially expressed among the four experimental groups, both STZ-induced diabetes and duration had a significant effect on the expression of 100 spots. For an additional 51 spots, STZ-induced diabetes resulted in significant changes in expression, whereas time had no effect. On the other hand, time had a significant effect on the expression of the remaining 19 spots, but STZ-induced diabetes did not. STZ-induced diabetes and time had a synergistic effect on the expression of 21 of the 100 spots. In this way, we were able to distinguish the spots that were changing due to time but not treatment, due to treatment but not time, and due to both in concert.

A total of 170 spots were excised from the preparative gel that was loaded with 500 μg of total protein, and these spots were in-gel digested for the subsequent MALDI-TOF and/or LTQ MS/MS analyses. Of this list, 162 spots were successfully sequenced, whereas the digest for the remaining eight

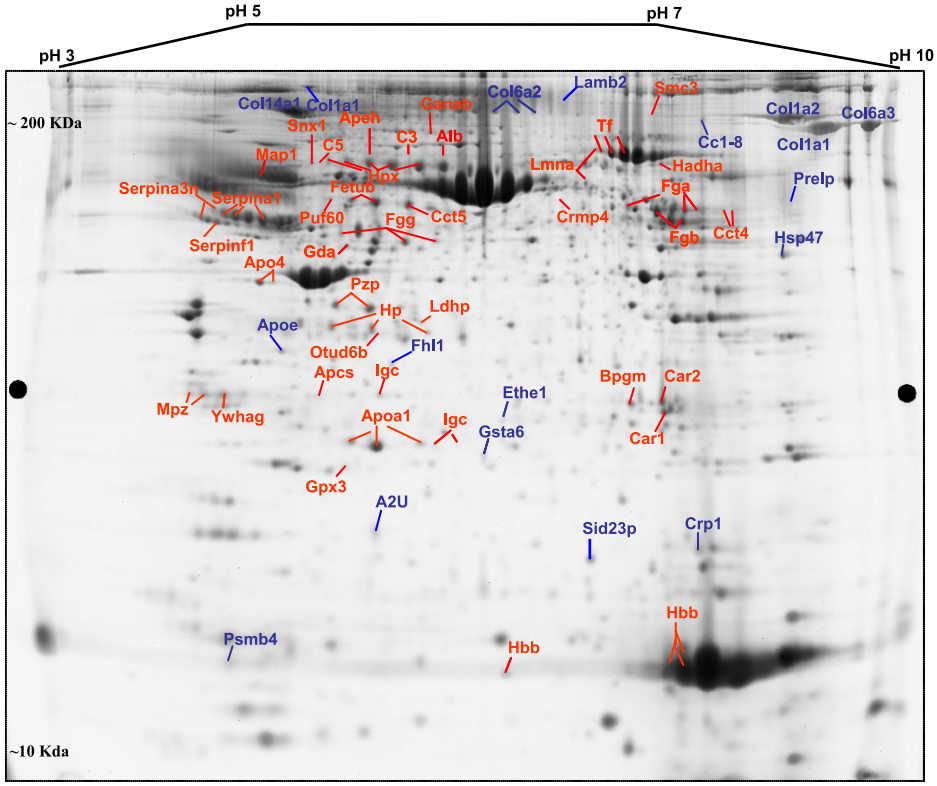

FIG. 2. **2D map of deep purple-labeled corpora tissue proteins indicating pick location of subset of proteins that changed in response to STZ-induced diabetes.** Orientation of the pH gradients is indicated on the *horizontal axes* from 3 (*left*) to 10 pH unit (*right*), and approximate apparent molecular mass ranges are indicated along the *vertical axes* from 10 (*bottom*) to 200 kDa (*top*).

spots did not reveal any peptides. A total of 90 spots were isoforms for 21 proteins due to either post-translational modification or proteolysis. As the overall expression patterns of the observed isoforms were similar, duplicates were omitted from the list in supplemental Table 1. Moreover, for 36 spots, more than one protein per spot passed our stringent filtering criteria, and the results for these spots were excluded from the list (supplemental Table 1) because the average ratio observed corresponds to the combination of all the proteins present for a particular spot, and individual changes are not conclusive to date. Thus, we report a total of 57 unique proteins along with the -fold changes that are summarized in supplemental Table 1 and detailed identification information in supplemental Tables 2 and 3 and supplemental Fig. 1, a–g.

A 2D map of a representative deep purple-stained gel is shown in Fig. 2. On this map, the pick locations of proteins whose expression is significantly different based on the variance of the mean change among the group ($p \leq 0.05$) are shown. In some cases, the same protein was identified in different spots across the 2D gel, suggesting the occurrence of post-translational modifications.

Principal Component Analysis—Global relationships among samples were visualized by performing a principal component analysis on the expression data (Fig. 3). Before dimensional reduction, each spot map existed in multidimensional space (one dimension for each of the expression values for a spot). The spot map comparisons were plotted in two-dimensional space, corresponding to the first and second principal components of variation. The first principal component for each spot map is the weighted linear combination of intensity values that shows maximum variation, whereas the second principal component is a weighted linear combination orthogonal to the first component that has maximum variance. For the 170 spots, the first principal component distinguished 71.1% of the variance with 9.7% additional variation distinguished by the second principal component. The PCA demonstrated that the 15 biological samples generally segregated into four groups, indicating that both diabetes and duration of diabetes are the primary factors affecting the differential expression of the proteins (supplemental Table 1). It is also clear that, within the diabetes group at both early (1 week) and late time points (2 months), the variance contributed by the inherent differences between the rats is larger compared with that of the control group, suggesting that there may be phenotype differences in the response to diabetes. One would not expect the individual samples to cluster in a way our experimental groups are clustered (shown in Fig. 3) if the -fold changes for the individual proteins reported in supplemental Table 1 arose by chance. In this way, the PCA further demonstrated the statistical significant of the -fold changes for the proteins reported in supplemental Table 1.

Differentially Expressed Proteins—The changes we report as significant (boldface font, supplemental Table 1) are for the proteins that have a $\geq$1.5- or ≤ -1.5-fold change in expression in the diabetic compared with the AMC. A total of 57 unique proteins are in this category. Eleven of these exhibited

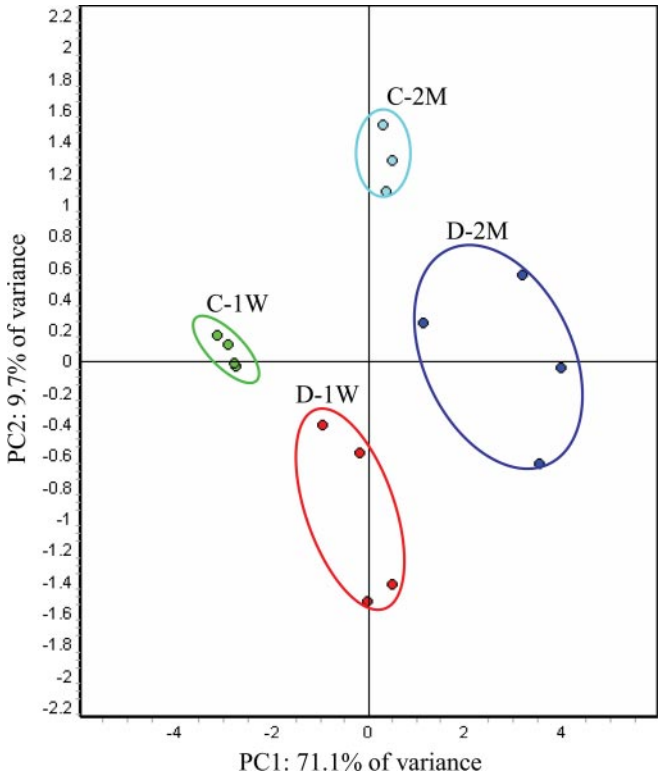

FIG. 3. **PCA of proteins mediated by STZ-induced diabetes.** The protein expression profiles of experimental groups were visualized in two-dimensional Euclidian space by using the extended data analysis module of DeCyder software as described under "Materials and Methods." The PCA distinctly clustered the 15 individual samples into four experimental groups (*C-1W*, 1-week control; *D-1W*, 1-week diabetes; *C-2M*, 2-month control; and *D-2M*, 2-month diabetes).

temporally significant changes 1 week after but not 2 months after STZ-induced diabetes and no change during the progression of the disease. In addition, 17 proteins showed significant changes starting 1 week after the induction of STZ diabetes and remained significant at 2 months. Although the directions of the -fold changes for these proteins at both 1 week and 2 months after STZ-induced diabetes are similar, the magnitudes for most of the proteins showed an ongoing increase from the 1-week to 2-month time point, emphasizing the progressive effects of the disease. Thus, these proteins represent potential early markers of diabetic complications. Significant changes for the remaining 25 proteins occurred only after 2 months of STZ treatment and the attendant hyperglycemia. The remaining four proteins showed age- but not diabetes-mediated significant -fold changes.

To understand the relationship of these proteins and their significance in the context of diabetes-associated organ dysfunction, to identify common transcriptional regulators, and to ascertain their interactions with other proteins in known networks, the identified proteins were analyzed using MetaCore analysis tools (47, 48). Of the total 57 proteins imported into the MetaCore, 53 were successfully mapped to the MetaCore database. A network of these proteins was generated using a "shortest paths algorithm." Protein-protein interaction networks among the proteins identified by 2D DIGE/MS and proteins from the MetaCore database are shown in Fig. 4. The proteins that were unconnected in the network were omitted. On this network, *nodes* (proteins) with the additional overlaid *red* and *blue circles* are proteins identified with 2D DIGE/MS in this study. The *red* and the *blue* colors of the *circles* represent the direction of the changes in the protein expression, up (*red*) and down (*blue*), with STZ-induced diabetes. The *edges* with *arrowheads* describe the nature and direction of the interaction. The *colored hexagons* on the *edge* describe the mechanism and the effect of interaction between proteins on the network: *green* for activation, *red* for inhibition, and *black* for unspecified.

For instance, according to this network (Fig. 4), STZ-induced diabetes increases abundance of a number of proteins that are regulated by common transcriptional factors such as p53 and c-Myc. Although none of these transcriptional factors were specifically detected with 2D DIGE/MS experiments, the nodes around these transcriptional factors were identified by 2D DIGE/MS and showed a consistent up- and down-regulation in agreement with the predicted interactions on the network. Thus, the networks pointed toward these core transcriptional factors and binding proteins that hypothetically could be involved in diabetes-mediated erectile dysfunction but might have been unnoticed based solely on the list of proteins identified by 2D DIGE/MS (supplemental Table 1).

To understand the biological relevance of the differentially expressed proteins and their -fold change implications in the context of diabetes-associated erectile dysfunction, the list of proteins with their expression data was visualized on MetaCore pre-existing pathway maps. The result of this mapping revealed the involvements of a number of proteins in the IL-6-mediated inflammation pathway map.

Validation by Immunoblotting—To further evaluate the nature and importance of the observed changes in protein expression listed in supplemental Table 1, some of the critical transcriptional factors that were identified by network analysis were selected for semiquantitative immunoblotting. This list of targets includes p53 and HDAC1. The relative -fold changes for these proteins were computed using ImageQuant-TL v2005 software and are summarized in Table II. At both the 1-week and 2-month time periods, the relative abundance of p53 increased by about 1.5-fold in STZ-induced diabetic compared with AMCs (Fig. 5), whereas the relative abundance of HDAC1 exhibited no significant change. As the immunoblot results for p53 are consistent with the network analysis prediction, this suggests that diabetes-mediated induction of Serpina3n and laminA could be regulated through hyperglycemia-mediated induction of p53.

To validate both the direction and the -fold changes identified by the 2D DIGE, representative proteins were selected on the basis of availability of high quality antibodies. These include Hsp47, 14-3-3-γ, and MPZ. Western blots, shown in

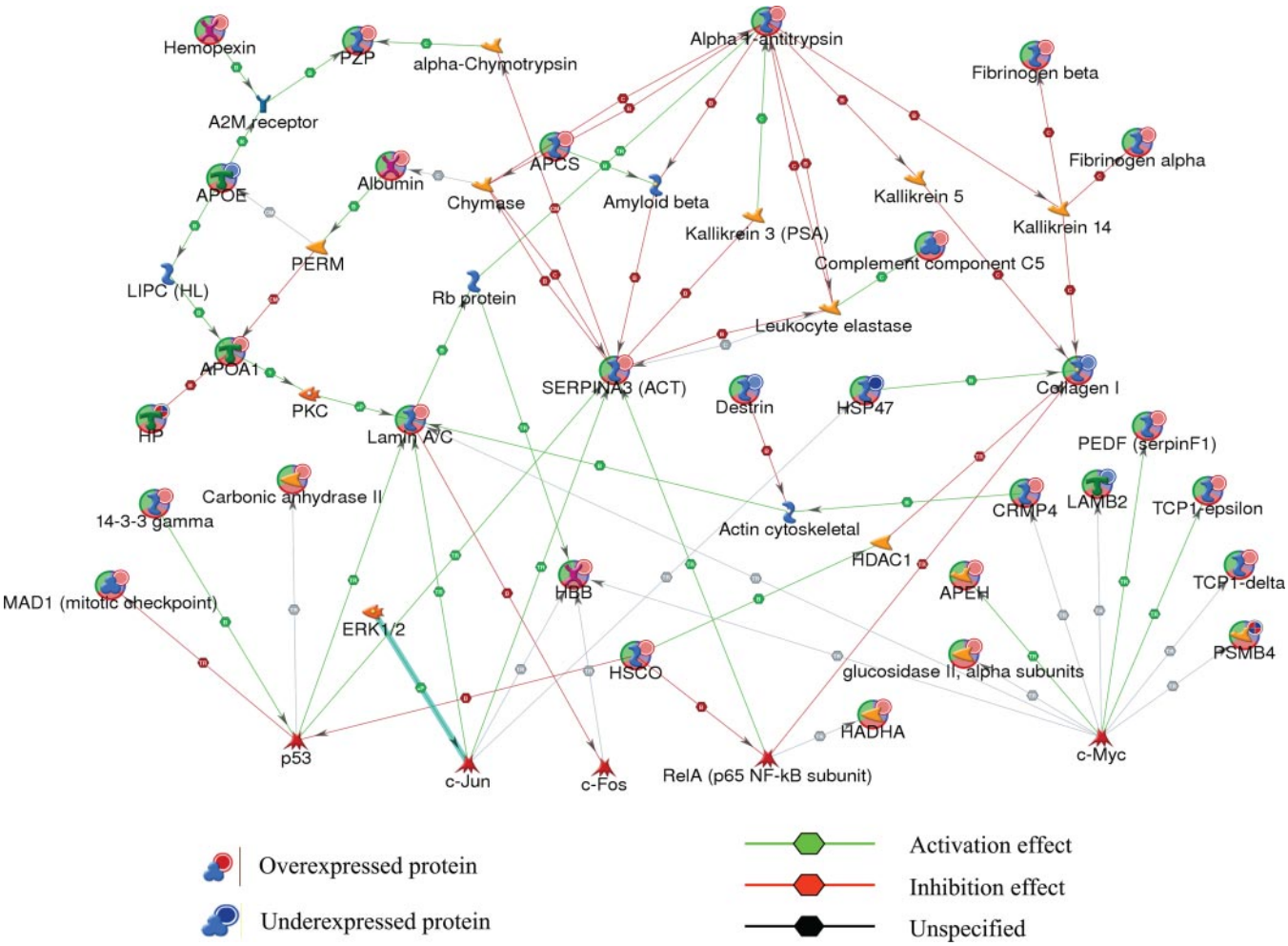

FIG. 4. **Protein networks associated with proteins differentially expressed in response to STZ-induced diabetes.** The network was generated by the shortest paths algorithm of MetaCore (GeneGo) software using the list of differentially expressed proteins identified by 2D DIGE/MS analysis. Individual proteins are represented as *nodes*, and the different *shapes* of the nodes represent the functional class of the proteins. The *edges* define the relationships of the nodes: the *arrowheads* indicate the direction of the interaction. *P* indicates phosphorylation, *T* indicates transformation, *B* indicates binding, *C* indicates cleavage, and *TR* indicates transcriptional regulation. The *color* of the *hexagons* on *edges* between *nodes* describes activation (*green*), inhibition (*red*), and unspecified (*black*) interactions. *PKC*, protein kinase C; Apeh, acyl-peptide hydrolase; apoE, apolipoprotein E precursor; Apcs, serum amyloid P component; Pzp, pregnancy-zone protein; HSCO/ETHE1, ethylmalonic encephalopathy 1; LIPC, hepatic triglyceride lipase; c-Jun, jun oncogene; c-Fos, FBJ osteosarcoma oncogene; c-Myc, myelocytomatosis oncogene; Hadha, mitochondrial trifunctional protein, alpha subunit; Hbb, hemoglobin subunit beta-1; Hp, haptoglobin.

TABLE II

Relative -fold changes for selected proteins that were identified by 2D DIGE/MS and/or by network analysis as determined by confirmational immunoblot analysis

Proteins	STZ-induced diabetic/control[a]	
	1 week	2 months
Hsp47	−2.8 ± 0.0013	−∞ ± 0.0197
p53[b]	1.20 ± 0.04	1.50 ± 0.013
14-3-3-γ	1.68 ± 0.0017	1.57 ± 0.0027
HDAC1[b]	1.29 ± 0.08	1.16 ± 0.031
MPZ	1.08 ± 0.11	1.17 ± 0.14
β-Actin	1.01 ± 0.0124	1.08 ± 0.0373

[a] Average of immunoblots from two independent biological replicates of STZ-induced diabetic rat model or age-matched control.

[b] Selected proteins that were identified by the network analysis.

Fig. 6, verified that both the direction and -fold changes for Hsp47 and 14-3-3-γ are consistent with the 2D DIGE results. For MPZ, even though 2D DIGE analysis showed diabetes-mediated -fold changes at both 1 week and 2 months after the induction of the diabetes, no change was confirmed with Western blot analysis. The fact that MPZ was identified in the acidic region on the gel relative to its pI (9.8) strongly suggests a diabetes-mediated post-translational modification for this protein, particularly those modifications that involve addition or loss of one or more charges to the amino acid chains. If this supposition is correct, the total amount of MPZ is not necessarily changing, consistent with the Western blot. Despite this discrepancy for MPZ, immunoblotting confirmed the quantitative results for rep-

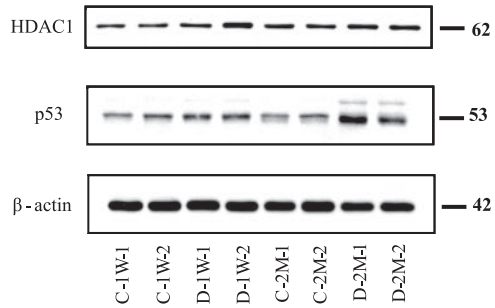

FIG. 5. **Confirmational immunoblots for selected proteins that were hypothetically identified by network analysis.** Each lane was loaded with a sample from an independent biological replicate (n = 2/experimental group). The blots were probed with antibodies to the proteins indicated at the *left*. *C-1W*, 1-week control; *D-1W*, 1-week diabetes; *C-2M*, 2-month control; and *D-2M*, 2-month diabetes.

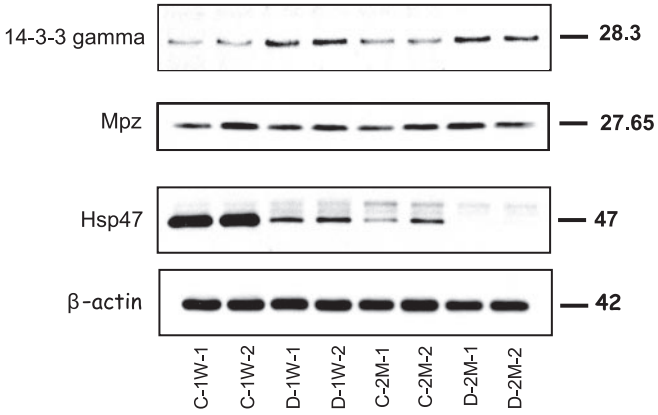

FIG. 6. **Confirmational immunoblots for selected proteins that were identified as differentially expressed by 2D DIGE.** An equal amount of total protein was loaded in each lane, and the resulting blots were probed with anti-Hsp47, anti-14-3-3-γ, and anti-MPZ. Relative -fold changes for these proteins in STZ-induced diabetic rats compared with the age-matched controls are given in Table II. *C-1W*, 1-week control; *D-1W*, 1-week diabetes; *C-2M*, 2-month control; and *D-2M*, 2-month diabetes.

resentative proteins that were detected by the 2D DIGE as well as obtained by theoretical prediction by network analysis.

DISCUSSION

Diabetes mellitus causes changes in the physiology and morphology of the erectile apparatus. To understand the possible causes of these changes at the proteome level during the initiation and progression of the disease, we identified changes in expression for multiple proteins at two time points after initiation of diabetes by treating an animal with STZ. The 1-week time point represents a period of hyperglycemia without significant effects on erectile function, whereas the 2-month time point represents a period of hyperglycemia that results in significant erectile dysfunction. Although STZ has toxic side effects that involve DNA alkylation (51) besides its effect on insulin production causing hyperglycemia, the results here are consistent with our previous findings (42) that very few proteins are significantly changed in abundance 1 week after the administration of STZ compared with the 2-month time point. This suggests that the effect of STZ toxicity on protein expression is limited compared with the effects of an extended period of hyperglycemia.

Down-regulated Proteins—We have recently shown a significant suppression of the different forms of collagen in diabetes bladder compared with age-matched controls (42). In this report, we show that both Hsp47 and the different forms of collagen are down-regulated by diabetes in corpora tissue. Our results are consistent with recent reports by both Sullivan *et al.* (32) and Hipp *et al.* (33) revealing that gene transcripts encoding components of collagen types 1, 2, 5, 6, and 11 in bladder and corpora smooth muscles are down-regulated in diabetic animal models when compared with controls. In agreement with these previous findings, different isoforms of collagen such as Col1a1 and Col1a2, both of which encode fibril-forming collagen type 1, which provides tissue both stiffness and tensile strength, were significantly down-regulated in corporal tissue at both 1 week and 2 months after the induction of diabetes. Although the possible mechanism by which collagen mediates erectile function has yet to be elucidated, the suppression of collagen in this diabetes model animals could contribute to the structural changes that have been demonstrated in both impotent patients and diabetic rats (52, 53). The 2D DIGE analysis results (supplemental Table 1) also demonstrated both a treatment- and a time-dependent down-regulation for Hsp47. In agreement with the 2D DIGE, a validation analysis by Western blot for this protein (shown in Fig. 6) showed both a treatment- and time-mediated down-regulation for this protein in the rat model. There is strong evidence demonstrating the importance of Hsp47 in collagen biosynthesis: Hsp47-null mice die before birth, and the embryos display ruptured blood vessels and a marked reduction in the amount of mature type 1 collagen (54). The exact mechanism by which Hsp47 contributes to the production of procollagen is unclear. However, several possible roles have been proposed, including acting as a molecular chaperone facilitating the folding and assembly of procollagen molecules, retaining unfolded molecules within the endoplasmic reticulum, and assisting the transport of correctly folded molecules from the endoplasmic reticulum to the Golgi apparatus (55). Changes in Hsp47 transcript levels often change in parallel with changes in collagen-specific gene expression, potentially implying that unknown co-regulation mechanisms exist (56). The synchronized down-regulation of the different forms of collagen (listed in supplemental Table 1) and Hsp47 certainly suggests that alterations in collagen biosynthesis and/or composition could contribute to the development of ED in the animal model. This overall down-regulation is opposite to observations in the diabetic kidney (57–59) in which it has been shown that for both type 1 and 2 diabetes there are increases in the different forms of collagen and Hsp47. The molecular basis for a diabetes-mediated tissue-specific down-regulation of both Hsp47 and

the different isoforms of collagens at both the transcriptional (32, 33) and translational levels (Ref. 42 and this study) has yet to be determined. In addition, future studies are required to determine whether the association between suppression of both Hsp47 and different forms of collagen and diabetes-mediated erectile dysfunction is causal.

Aside from these results on collagen, androgen-regulated proteins, including cystatin-related protein 1 (CRP1) and α-2u-globulin (A2U), are down-regulated in this rat model. CRP, originally described as androgen-regulated 20- or 22-kDa glycoprotein (60, 61), has been called CRP because of its marked sequence homology to cystatin (62, 63). The function of CRP is still unknown, and no protease inhibitory activity has yet been demonstrated. CRP1 is expressed and androgen-regulated in organs that contain relatively higher levels of androgen receptors (64, 65). Similarly, an early study by Roy and co-workers (66, 67) has shown that the synthesis of A2U in the hepatic parenchymal cells is induced *in vivo* by androgen, glucocorticoid growth hormone, and insulin and inhibited by estrogen. In contrast, constitutive expression for α-2u-globulin has been demonstrated in the salivary and lachrymal glands (68). Thus, expression of A2U mRNA is regulated under different developmental and hormonal levels in different tissues (68). α-2u-globulin, a close homologue of mouse major urinary protein, accounts for about half of the total excreted protein in adult male rat urine but is absent from the urine of females. There is indirect evidence that α-2u-globulin functions in pheromone transport (69), but its exact physiological role has yet to be illustrated. This is consistent with its observed binding properties, its close similarity with major urinary protein, and the known properties of male rat urine. Down-regulation of these proteins in diabetic corpora is consistent with previous findings where androgen deficiency has been shown to suppress the expression of these proteins (66, 67). Our results suggest that in diabetic erectile tissue of model animals and/or patients suppression of these proteins could be mediated through circulating androgen levels. It is generally accepted that androgens are critical for development, growth, and maintenance of penile erectile tissue. In addition, androgen deficiency impairs NO-dependent relaxation of the penile tissue (14, 70, 71). This reduced vascular reactivity appears to be due to deficiency of androgenic action that is exerted at the genomic level, modulating the expression of the neuronal form of the nitric-oxide synthase gene (20, 70, 71).

Up-regulated Proteins—As described under "Results," a network of differentially expressed proteins was generated using the MetaCore network analysis tool to help identify common transcriptional regulators. It is shown (Fig. 4) that a significant number of proteins that were up-regulated in response to an STZ-induced hyperglycemia are co-regulated by the major transcriptional regulators p53 and c-Myc. Parallel induction of c-Myc-regulated targets, including Cct4, Cct5, and pigment epithelium-derived factor (PEDF), along with p53 has recently been associated with the induction of β-cell apoptosis in STZ- and/or glucosamine-treated β-cell and/or human umbilical vein endothelial cells (72, 73). Increases in apoptosis have been linked to a spectrum of diabetic complications (74–76). Consistent with this report, the parallel induction of Cct4 and Cct5 as well as p53 in STZ-treated diabetic rat could be directly associated with the significant decreases seen in the numbers of smooth muscle cells in diabetic corpora tissue (77). Moreover, 14-3-3-γ, which is known to activate the DNA binding affinity of p53 upon stress by binding to a C-terminal domain containing a phosphorylated serine, is also up-regulated with diabetes. Both the phosphorylation status at serine and 14-3-3-γ binding were shown to be critical events for human p53 to be functional (78). These results support the notion that hyperglycemia with diabetes promotes cell apoptosis mediated by both induction and activation of p53.

In addition, the growth regulatory function of p53 through stress-dependent cellular export of growth-inhibitory stimuli from damaged cells to neighboring tissue with γ irradiation or chemotherapeutic treatment has been reported (79). On the list of the growth-inhibitory stimuli reported, the various serine protease inhibitors are included. The induction of p53 and the different forms of serine protease inhibitors such as Serpina1 and Serpina3n in this diabetic animal model could indicate smooth muscle cell damage progression mediated by hyperglycemia. Thus, the progressive loss of normal cavernosal endothelium and smooth muscle cells from corpus cavernosum as disease progresses (1, 80) could also be mediated through p53-dependent secretion of growth inhibitors that may affect proliferating cells and lead to a gradual decrease in the overall proliferative capacity of corporal tissue. Parallel with the induction of p53, α_2-antiplasmin (Serpinf1) also known as PEDF is up-regulated with diabetes. Serpinf1 is a potent angiogenic inhibitor, and increased serum levels of Serpinf1 in both type 1 and type 2 diabetic patients have been reported (81, 82). Recently Ho *et al.* (73) demonstrated sequential expression of peroxisome proliferator-activated receptor γ and p53 with PEDF using immunoblotting and immunofluorescence assays in human umbilical vein endothelial cells. Although peroxisome proliferator-activated receptor γ was not identified in our study, we observed up-regulation of PEDF in parallel with p53. Overall, a parallel induction of p53 and proteins that are associated with the induction of p53 substantiates the idea that smooth muscle cells undergo apoptosis by a process dependent on the p53 tumor suppressor protein. This programmed cell death could be involved in the pathogenesis of poor diabetic corpora tissue responses to inflammation and ischemia and eventually contribute to target organ damage and dysfunction.

Proteins that are involved in lipid metabolism and also have been demonstrated to have anti-inflammatory responses, such as apoA-I and apoA-IV, showed significant increases starting from 1 week after the STZ-induced diabetes and remained increased at the 2-month time point of the disease

compared with the age-matched controls (83, 84). These increases in apoA-I and apoA-IV with a decrease in apoE are consistent with the previous reports in diabetic whole plasma (85, 86). The decreases in the level of apoE in STZ-induced diabetes may imply that apoE is probably attributable to the decreased lipid and/or lipoprotein metabolism associated with a decrease in the level of circulatory insulin in these diabetic model animals. On the other hand, apoA-I participates in the reverse transport of cholesterol from tissues to the liver for excretion by promoting cholesterol efflux from tissues and by acting as a cofactor for lecithin-cholesterol acyltransferase (87). In this way, the induction of apoA-I and apoA-IV in these diabetes model animals could be to restore lipid homeostasis by minimizing the rise in the level of lipids and lipoproteins in the circulating blood due to diabetes-induced suppression of apoE in the very low density lipoprotein particle (85). Therefore, the result from our study suggests the presence of major compositional changes in circulating lipoproteins that may contribute to defective triglyceride clearance from the circulation in these diabetes model animals. These are the types of changes that are expected if narrowing or hardening (atherogenesis) of the blood vessel occurs that could contribute to an interrupted blood supply to the penis or pelvic area and hence to organ dysfunction.

In humans, bisphosphoglycerate mutase is mainly present in the erythrocytes and plays a pivotal role in the dissociation of oxygen from Hb via 2,3-BPG. Bisphosphoglycerate mutase is one of the enzymes that undergoes glycation as a result of contact with high levels of blood glucose. A study by Fujita *et al.* (88) has shown a decreased specific activity of bisphosphoglycerate mutase in erythrocytes of diabetic patients compared with normal controls. They also demonstrated that the loss of enzymatic activity apparently is because of glycation of the enzyme at several lysine residues. The induction of this protein in the STZ diabetic rat model may therefore be a compensatory mechanism to restore the loss of the enzyme through glycation or to generate more 2,3-BPG, which might then stabilize the low oxygen affinity state of hemoglobin and make it harder for oxygen to bind hemoglobin and more likely to be released to adjacent tissues. Thus, as the 2,3-BPG is part of a feedback loop, its induction as well as the induction of Gpx3 can help prevent tissue hypoxia that is most likely to occur in diabetes.

Of the proteins that were up-regulated in this study, we report the induction of IgC (anti-NGF). However, decreases in the NGF level in both bladder and lumbosacral dorsal root ganglia (L6DRG) and also a direct correlation between deprivation of NGF and progression of diabetic cystopathy have been reported (89). This group has also demonstrated the reversal of the NGF level back to normal by injecting HSV-1 encoding NGF gene. In a different experiment, it was shown that less NGF is expressed in the penile tissue of older rats compared with younger rats (90). This implies that endogenous penile/cavernosal nerve repair may be reduced in older organisms and may contribute, at least in part, to the development of ED frequently seen in older age. However, induction of anti-NGF with diabetes in erectile tissue has not been revealed before. A decrease in the tissue level of NGF could be associated with the induction and neutralizing effect of anti-NGF with diabetes. Therefore, the induction of anti-NGF could counteract the biological activity of NGF in these diabetic model animals.

In summary, our results broaden the list of candidate proteins that have their expression changed in corporal tissue in response to diabetes. The changes in expression of these proteins could account for the functional deficits known to occur in erectile dysfunction or be a compensatory response to try to restore erectile function. Our results suggest that diabetes-mediated erectile dysfunction in this model involves down-regulation of proteins that provide tensile strength and stiffness of the corpora tissue and proteins associated with transport of sex hormones. There was up-regulation of proteins that are involved in p53-mediated smooth muscle cell apoptosis, which could be associated with cell damage and therefore contribute to erectile dysfunction. The candidate proteins that we identified in this study provide novel insights into diabetes-induced erectile dysfunction that can be explored in future studies and can possibly be used to identify diagnostic or drug targets. Expression analysis using the 2D DIGE/MS platform gave us statistically significant quantitative information from four biological replicate samples per experimental group on well over 57 proteins. However, there are certain limitations associated with both the corpora tissue and the 2D DIGE methodology that are worth discussion. Erectile tissues are relatively enriched with smooth muscle cells, but there are clearly mixtures of cell types in the harvested corpora samples. As a result, differential expressions for certain proteins that are especially common to both the corpora tissue and the circulating blood are contributed from different cell types. In addition, proteins outside the molecular range, hydrophobic proteins difficult to resolve using 2D gel techniques, and low abundance proteins could not be surveyed in this study. Nonetheless, this work demonstrates the importance of using 2D DIGE techniques to analyze proteome expression in well characterized tissues. In particular, the information provided on the effect of duration of diabetes on protein expression in the corpora may be valuable in identifying biomarkers that will predict disease progression in patients and targeting interventions to the correct patient subpopulation.

* This work was supported, in whole or in part, by National Institutes of Health Grants R21 DK-070229 and P01-DK060037 from the NIDDK.

S The on-line version of this article (available at http://www.mcponline.org) contains supplemental Fig. 1 and Tables 1–3.

‖ To whom correspondence should be addressed: Center for Proteomics and Bioinformatics, Dept. of Physiology and Biophysics, 930 BRB School of Medicine, Case Western Reserve University, 10900 Euclid Ave., Cleveland, OH 44106. Tel.: 216-368-4406; Fax: 216-368-3812; E-mail: mark.chance@case.edu.

REFERENCES

1. Burchardt, T., Burchardt, M., Karden, J., Buttyan, R., Shabsigh, A., de la Taille, A., Ng, P. Y., Anastasiadis, A. G., and Shabsigh, R. (2000) Reduction of endothelial and smooth muscle density in the corpora cavernosa of the streptozotocin induced diabetic rat. *J. Urol.* **164,** 1807–1811
2. Shabsigh, R., Klein, L. T., Seidman, S., Kaplan, S. A., Lehrhoff, B. J., and Ritter, J. S. (1998) Increased incidence of depressive symptoms in men with erectile dysfunction. *Urology* **52,** 848–852
3. Lue, T. F. (2000) Erectile dysfunction. *New Engl. J. Med.* **342,** 1802–1813
4. Feldman, H. A., Goldstein, I., Hatzichristou, D. G., Krane, R. J., and McKinlay, J. B. (1994) Impotence and its medical and psychosocial correlates: results of the Massachusetts Male Aging Study. *J. Urol.* **151,** 54–61
5. Rosen, R. C., Fisher, W. A., Eardley, I., Niederberger, C., Nadel, A., and Sand, M. (2004) The multinational Men's Attitudes to Life Events and Sexuality (MALES) study: I. Prevalence of erectile dysfunction and related health concerns in the general population. *Curr. Med. Res. Opin.* **20,** 607–617
6. Eardley, I., Fisher, W., Rosen, R. C., Niederberger, C., Nadel, A., and Sand, M. (2007) The multinational Men's Attitudes to Life Events and Sexuality study: the influence of diabetes on self-reported erectile function, attitudes and treatment-seeking patterns in men with erectile dysfunction. *Int. J. Clin. Pract.* **61,** 1446–1453
7. De Berardis, G., Franciosi, M., Belfiglio, M., Di Nardo, B., Greenfield, S., Kaplan, S. H., Pellegrini, F., Sacco, M., Tognoni, G., Valentini, M., and Nicolucci, A. (2002) Erectile dysfunction and quality of life in type 2 diabetic patients: a serious problem too often overlooked. *Diabetes Care* **25,** 284–291
8. Penson, D. F., Latini, D. M., Lubeck, D. P., Wallace, K. L., Henning, J. M., and Lue, T. F. (2003) Do impotent men with diabetes have more severe erectile dysfunction and worse quality of life than the general population of impotent patients? Results from the Exploratory Comprehensive Evaluation of Erectile Dysfunction (ExCEED) database. *Diabetes Care* **26,** 1093–1099
9. Brown, J. S., Wessells, H., Chancellor, M. B., Howards, S. S., Stamm, W. E., Stapleton, A. E., Steers, W. D., Van Den Eeden, S. K., and McVary, K. T. (2005) Urologic complications of diabetes. *Diabetes Care* **28,** 177–185
10. Guay, A. T., Perez, J. B., Jacobson, J., and Newton, R. A. (2001) Efficacy and safety of sildenafil citrate for treatment of erectile dysfunction in a population with associated organic risk factors. *J. Androl.* **22,** 793–797
11. Murray, F. T., Johnson, R. D., Sciadini, M., Katovich, M. J., Rountree, J., and Jewett, H. (1992) Erectile and copulatory dysfunction in chronically diabetic BB/WOR rats. *Am. J. Physiol. Endocrinol. Metab.* **263,** E151–E157
12. Bancroft, J., and Wu, F. C. (1983) Changes in erectile responsiveness during androgen replacement therapy. *Arch. Sex. Behav.* **12,** 59–66
13. Kwan, M., Greenleaf, W. J., Mann, J., Crapo, L., and Davidson, J. M. (1983) The nature of androgen action on male sexuality: a combined laboratory-self-report study on hypogonadal men. *J. Clin. Endocrinol. Metab.* **57,** 557–562
14. Vernet, D., Cai, L., Garban, H., Babbitt, M. L., Murray, F. T., Rajfer, J., and Gonzalez-Cadavid, N. F. (1995) Reduction of penile nitric oxide synthase in diabetic BB/WORdp (type I) and BBZ/WORdp (type II) rats with erectile dysfunction. *Endocrinology* **136,** 5709–5717
15. McVary, K. T., Rathnau, C. H., and McKenna, K. E. (1997) Sexual dysfunction in the diabetic BB/WOR rat: a role of central neuropathy. *Am. J. Physiol. Regul. Integr. Comp. Physiol.* **272,** R259–R267
16. El-Latif, M. A., Makhlouf, A. A., Moustafa, Y. M., Gouda, T. E., Niederberger, C. S., and Elhanbly, S. M. (2006) Diagnostic value of nitric oxide, lipoprotein(a), and malondialdehyde levels in the peripheral venous and cavernous blood of diabetics with erectile dysfunction. *Int. J. Impot. Res.* **18,** 544–549
17. Prieto, D. (2008) Physiological regulation of penile arteries and veins. *Int. J. Impot. Res.* **20,** 17–29
18. Chitaley, K., Wingard, C. J., Clinton Webb, R., Branam, H., Stopper, V. S., Lewis, R. W., and Mills, T. M. (2001) Antagonism of Rho-kinase stimulates rat penile erection via a nitric oxide-independent pathway. *Nat. Med.* **7,** 119–122
19. Farrell, J. B., Deshmukh, A., and Baghaie, A. A. (2008) Low testosterone and the association with type 2 diabetes. *Diabetes Educ.* **34,** 799–806
20. Zhang, X. H., Filippi, S., Morelli, A., Vignozzi, L., Luconi, M., Donati, S., Forti, G., and Maggi, M. (2006) Testosterone restores diabetes-induced erectile dysfunction and sildenafil responsiveness in two distinct animal models of chemical diabetes. *J. Sex. Med.* **3,** 253–264; discussion 264–265, author reply 265–266
21. Fushimi, H., Horie, H., Inoue, T., Kameyama, M., Kanao, K., Ishihara, S., Tsujimura, T., Nunotani, H., Minami, T., Okazaki, Y., and Tochino, Y. (1989) Low testosterone levels in diabetic men and animals: a possible role in testicular impotence. *Diabetes Res. Clin. Pract.* **6,** 297–301
22. Saenz de Tejada, I., Goldstein, I., Azadzoi, K., Krane, R. J., and Cohen, R. A. (1989) Impaired neurogenic and endothelium-mediated relaxation of penile smooth muscle from diabetic men with impotence. *New Engl. J. Med.* **320,** 1025–1030
23. Cohen, R. A. (2005) Role of nitric oxide in diabetic complications. *Am. J. Ther.* **12,** 499–502
24. Cartledge, J. J., Eardley, I., and Morrison, J. F. (2001) Advanced glycation end-products are responsible for the impairment of corpus cavernosal smooth muscle relaxation seen in diabetes. *BJU Int.* **87,** 402–407
25. Seftel, A. D., Vaziri, N. D., Ni, Z., Razmjouei, K., Fogarty, J., Hampel, N., Polak, J., Wang, R. Z., Ferguson, K., Block, C., and Haas, C. (1997) Advanced glycation end products in human penis: elevation in diabetic tissue, site of deposition, and possible effect through iNOS or eNOS. *Urology* **50,** 1016–1026
26. Bivalacqua, T. J., Hellstrom, W. J., Kadowitz, P. J., and Champion, H. C. (2001) Increased expression of arginase II in human diabetic corpus cavernosum: in diabetic-associated erectile dysfunction. *Biochem. Biophys. Res. Commun.* **283,** 923–927
27. Cartledge, J. J., Eardley, I., and Morrison, J. F. (2001) Nitric oxide-mediated corpus cavernosal smooth muscle relaxation is impaired in ageing and diabetes. *BJU Int.* **87,** 394–401
28. Sullivan, M. E., Mumtaz, F. H., Dashwood, M. R., Thompson, C. S., Naseem, K. M., Bruckdorfer, K. R., Mikhailidis, D. P., and Morgan, R. J. (2002) Enhanced relaxation of diabetic rabbit cavernosal smooth muscle in response to nitric oxide: potential relevance to erectile dysfunction. *Int. J. Impot. Res.* **14,** 523–532
29. Kloner, R. A., and Speakman, M. (2002) Erectile dysfunction and atherosclerosis. *Curr. Atheroscler. Rep.* **4,** 397–401
30. Montorsi, P., Ravagnani, P. M., Galli, S., Rotatori, F., Briganti, A., Salonia, A., Dehò, F., and Montorsi, F. (2004) Common grounds for erectile dysfunction and coronary artery disease. *Curr. Opin. Urol.* **14,** 361–365
31. Kapur, V., and Schwarz, E. R. (2007) The relationship between erectile dysfunction and cardiovascular disease. Part I: pathophysiology and mechanisms. *Rev. Cardiovasc. Med.* **8,** 214–219
32. Sullivan, C. J., Teal, T. H., Luttrell, I. P., Tran, K. B., Peters, M. A., and Wessells, H. (2005) Microarray analysis reveals novel gene expression changes associated with erectile dysfunction in diabetic rats. *Physiol. Genomics* **23,** 192–205
33. Hipp, J. D., Davies, K. P., Tar, M., Valcic, M., Knoll, A., Melman, A., and Christ, G. J. (2007) Using gene chips to identify organ-specific, smooth muscle responses to experimental diabetes: potential applications to urological diseases. *BJU Int.* **99,** 418–430
34. Andersson, K. E. (2003) Erectile physiological and pathophysiological pathways involved in erectile dysfunction. *J. Urol.* **170,** S6–S13; discussion S13–S14
35. Rehman, J., Chenven, E., Brink, P., Peterson, B., Walcott, B., Wen, Y. P., Melman, A., and Christ, G. (1997) Diminished neurogenic but not pharmacological erections in the 2- to 3-month experimentally diabetic F-344 rat. *Am. J. Physiol. Heart Circ. Physiol.* **272,** H1960–H1971
36. Christ, G. J., Hsieh, Y., Zhao, W., Schenk, G., Venkateswarlu, K., Wang, H. Z., Tar, M. T., and Melman, A. (2006) Effects of streptozotocin-induced diabetes on bladder and erectile (dys)function in the same rat in vivo. *BJU Int.* **97,** 1076–1082
37. Lilley, K. S., and Friedman, D. B. (2004) All about DIGE: quantification technology for differential-display 2D-gel proteomics. *Expert Rev. Proteomics* **1,** 401–409
38. Alban, A., David, S. O., Bjorkesten, L., Andersson, C., Sloge, E., Lewis, S., and Currie, I. (2003) A novel experimental design for comparative two-dimensional gel analysis: two-dimensional difference gel electrophoresis incorporating a pooled internal standard. *Proteomics* **3,** 36–44
39. Friedman, D. B., Hill, S., Keller, J. W., Merchant, N. B., Levy, S. E., Coffey, R. J., and Caprioli, R. M. (2004) Proteome analysis of human colon

cancer by two-dimensional difference gel electrophoresis and mass spectrometry. *Proteomics* **4,** 793–811
40. Friedman, D. B., and Lilley, K. S. (2008) Optimizing the difference gel electrophoresis (DIGE) technology. *Methods Mol. Biol.* **428,** 93–124
41. Marouga, R., David, S., and Hawkins, E. (2005) The development of the DIGE system: 2D fluorescence difference gel analysis technology. *Anal. Bioanal. Chem.* **382,** 669–678
42. Yohannes, E., Chang, J., Christ, G. J., Davies, K. P., and Chance, M. R. (2008) Proteomics analysis identifies molecular targets related to diabetes mellitus-associated bladder dysfunction. *Mol. Cell. Proteomics* **7,** 1270–1285
43. Chang, J., Chance, M. R., Nicholas, C., Ahmed, N., Guilmeau, S., Flandez, M., Wang, D., Byun, D. S., Nasser, S., Albanese, J. M., Corner, G. A., Heerdt, B. G., Wilson, A. J., Augenlicht, L. H., and Mariadason, J. M. (2008) Proteomic changes during intestinal cell maturation in vivo. *J. Proteomics* **71,** 530–546
44. Nibbe, R. K., Markowitz, S., Myeroff, L., Ewing, R., and Chance, M. R. (2009) Discovery and scoring of protein interaction subnetworks discriminative of late stage human colon cancer. *Mol. Cell. Proteomics* **8,** 827–845
45. Weissman, B. A., Niu, E., Ge, R., Sottas, C. M., Holmes, M., Hutson, J. C., and Hardy, M. P. (2005) Paracrine modulation of androgen synthesis in rat Leydig cells by nitric oxide. *J. Androl.* **26,** 369–378
46. Zheng, L., Liu, S., Sun, M. Z., Chang, J., Chance, M. R., and Kern, T. S. (2009) Pharmacologic intervention targeting glycolytic-related pathways protects against retinal injury due to ischemia and reperfusion. *Proteomics* **9,** 1869–1882
47. Nikolsky, Y., Ekins, S., Nikolskaya, T., and Bugrim, A. (2005) A novel method for generation of signature networks as biomarkers from complex high throughput data. *Toxicol. Lett.* **158,** 20–29
48. Mason, C. W., Swaan, P. W., and Weiner, C. P. (2006) Identification of interactive gene networks: a novel approach in gene array profiling of myometrial events during guinea pig pregnancy. *Am. J. Obstet. Gynecol.* **194,** 1513–1523
49. Davies, K. P., Zhao, W., Tar, M., Figueroa, J. C., Desai, P., Verselis, V. K., Kronengold, J., Wang, H. Z., Melman, A., and Christ, G. J. (2007) Diabetes-induced changes in the alternative splicing of the slo gene in corporal tissue. *Eur. Urol.* **52,** 1229–1237
50. Shevchenko, A., Wilm, M., Vorm, O., and Mann, M. (1996) Mass spectrometric sequencing of proteins silver-stained polyacrylamide gels. *Anal. Chem.* **68,** 850–858
51. Bennett, R. A., and Pegg, A. E. (1981) Alkylation of DNA in rat tissues following administration of streptozotocin. *Cancer Res.* **41,** 2786–2790
52. Yaman, O., Yilmaz, E., Bozlu, M., and Anafarta, K. (2003) Alterations of intracorporeal structures in patients with erectile dysfunction. *Urol. Int.* **71,** 87–90
53. Salama, N., and Kagawa, S. (1999) Ultra-structural changes in collagen of penile tunica albuginea in aged and diabetic rats. *Int. J. Impot. Res.* **11,** 99–105
54. Nagata, K. (2003) HSP47 as a collagen-specific molecular chaperone: function and expression in normal mouse development. *Semin. Cell Dev. Biol.* **14,** 275–282
55. Nagata, K. (1996) Hsp47: a collagen-specific molecular chaperone. *Trends Biochem. Sci.* **21,** 22–26
56. Rocnik, E. F., van der Veer, E., Cao, H., Hegele, R. A., and Pickering, J. G. (2002) Functional linkage between the endoplasmic reticulum protein Hsp47 and procollagen expression in human vascular smooth muscle cells. *J. Biol. Chem.* **277,** 38571–38578
57. Liu, D., Razzaque, M. S., Cheng, M., and Taguchi, T. (2001) The renal expression of heat shock protein 47 and collagens in acute and chronic experimental diabetes in rats. *Histochem. J.* **33,** 621–628
58. Razzaque, M. S., Kumatori, A., Harada, T., and Taguchi, T. (1998) Coexpression of collagens and collagen-binding heat shock protein 47 in human diabetic nephropathy and IgA nephropathy. *Nephron* **80,** 434–443
59. Ohashi, S., Abe, H., Takahashi, T., Yamamoto, Y., Takeuchi, M., Arai, H., Nagata, K., Kita, T., Okamoto, H., Yamamoto, H., and Doi, T. (2004) Advanced glycation end products increase collagen-specific chaperone protein in mouse diabetic nephropathy. *J. Biol. Chem.* **279,** 19816–19823
60. Wang, T. Y., Chamberlin, L. L., and Xu, Y. H. (1986) Characterization of the androgen-dependent 22Kdalton glycoprotein from rat ventral prostate. *J. Steroid Biochem.* **24,** 929–932
61. Chamberlin, L. L., Mpanias, O. D., and Wang, T. Y. (1983) Isolation, properties, and androgen regulation of a 20-kilodalton protein from rat ventral prostate. *Biochemistry* **22,** 3072–3077
62. Devos, A., Claessens, F., Alen, P., Winderickx, J., Heyns, W., Rombauts, W., and Peeters, B. (1997) Identification of a functional androgen-response element in the exon 1-coding sequence of the cystatin-related protein gene crp2. *Mol. Endocrinol.* **11,** 1033–1043
63. Winderickx, J., Hemschoote, K., De Clercq, N., Van Dijck, P., Peeters, B., Rombauts, W., Verhoeven, G., and Heyns, W. (1990) Tissue-specific expression and androgen regulation of different genes encoding rat prostatic 22-kilodalton glycoproteins homologous to human and rat cystatin. *Mol. Endocrinol.* **4,** 657–667
64. Vanaken, H., Claessens, F., Vercaeren, I., Heyns, W., Peeters, B., and Rombauts, W. (1996) Androgenic induction of cystatin-related protein and the C3 component of prostatic binding protein in primary cultures from the rat lacrimal gland. *Mol. Cell. Endocrinol.* **121,** 197–205
65. Vercaeren, I., Vanaken, H., Devos, A., Peeters, B., Verhoeven, G., and Heyns, W. (1996) Androgens transcriptionally regulate the expression of cystatin-related protein and the C3 component of prostatic binding protein in rat ventral prostate and lacrimal gland. *Endocrinology* **137,** 4713–4720
66. Roy, A. K., and Leonard, S. (1973) Androgen-dependent synthesis of 2u globulin in diabetic rats: the role of insulin. *J. Endocrinol.* **57,** 327–328
67. Murty, C. V., Rao, K. V., and Roy, A. K. (1987) Rapid androgenic stimulation of alpha 2u-globulin synthesis in the perfused rat liver. *Endocrinology* **121,** 1814–1818
68. Gubits, R. M., Lynch, K. R., Kulkarni, A. B., Dolan, K. P., Gresik, E. W., Hollander, P., and Feigelson, P. (1984) Differential regulation of alpha 2u globulin gene expression in liver, lachrymal gland, and salivary gland. *J. Biol. Chem.* **259,** 12803–12809
69. Böcskei, Z., Groom, C. R., Flower, D. R., Wright, C. E., Phillips, S. E., Cavaggioni, A., Findlay, J. B., and North, A. C. (1992) Pheromone binding to two rodent urinary proteins revealed by X-ray crystallography. *Nature* **360,** 186–188
70. Traish, A., and Kim, N. (2005) The physiological role of androgens in penile erection: regulation of corpus cavernosum structure and function. *J. Sex. Med.* **2,** 759–770
71. Reilly, C. M., Zamorano, P., Stopper, V. S., and Mills, T. M. (1997) Androgenic regulation of NO availability in rat penile erection. *J. Androl.* **18,** 110–115
72. Park, J., Kwon, H., Kang, Y., and Kim, Y. (2007) Proteomic analysis of O-GlcNAc modifications derived from streptozotocin and glucosamine induced beta-cell apoptosis. *J. Biochem. Mol. Biol.* **40,** 1058–1068
73. Ho, T. C., Chen, S. L., Yang, Y. C., Liao, C. L., Cheng, H. C., and Tsao, Y. P. (2007) PEDF induces p53-mediated apoptosis through PPAR gamma signaling in human umbilical vein endothelial cells. *Cardiovasc. Res.* **76,** 213–223
74. Jazayeri, L., Callaghan, M. J., Grogan, R. H., Hamou, C. D., Thanik, V., Ingraham, C. R., Capell, B. C., Pelo, C. R., and Gurtner, G. C. (2008) Diabetes increases p53-mediated apoptosis following ischemia. *Plast. Reconstr. Surg.* **121,** 1135–1143
75. Allen, D. A., Yaqoob, M. M., and Harwood, S. M. (2005) Mechanisms of high glucose-induced apoptosis and its relationship to diabetic complications. *J. Nutr. Biochem.* **16,** 705–713
76. Ryan, A., Murphy, M., Godson, C., and Hickey, F. B. (2009) Diabetes mellitus and apoptosis: inflammatory cells. *Apoptosis* **14,** 1435–1450
77. Xie, D., Odronic, S. I., Wu, F., Pippen, A., Donatucci, C. F., and Annex, B. H. (2007) Mouse model of erectile dysfunction due to diet-induced diabetes mellitus. *Urology* **70,** 196–201
78. Rajagopalan, S., Jaulent, A. M., Wells, M., Veprintsev, D. B., and Fersht, A. R. (2008) 14-3-3 activation of DNA binding of p53 by enhancing its association into tetramers. *Nucleic Acids Res.* **36,** 5983–5991
79. Komarova, E. A., Diatchenko, L., Rokhlin, O. W., Hill, J. E., Wang, Z. J., Krivokrysenko, V. I., Feinstein, E., and Gudkov, A. V. (1998) Stress-induced secretion of growth inhibitors: a novel tumor suppressor function of p53. *Oncogene* **17,** 1089–1096
80. Fani, K., Lundin, A. P., Beyer, M. M., Jimenez, F. A., and Friedman, E. A. (1983) Pathology of the penis in long-term diabetic rats. *Diabetologia* **25,** 424–428

81. Nakamura, K., Yamagishi, S., Adachi, H., Kurita-Nakamura, Y., Matsui, T., and Inoue, H. (2009) Serum levels of pigment epithelium-derived factor (PEDF) are positively associated with visceral adiposity in Japanese patients with type 2 diabetes. *Diabetes Metab. Res. Rev.* **25,** 52–56
82. Jenkins, A., Zhang, S. X., Gosmanova, A., Aston, C., Dashti, A., Baker, M. Z., Lyons, T., and Ma, J. X. (2008) Increased serum pigment epithelium derived factor levels in Type 2 diabetes patients. *Diabetes Res. Clin. Pract.* **82,** e5–e7
83. Van Lenten, B. J., Wagner, A. C., Jung, C. L., Ruchala, P., Waring, A. J., Lehrer, R. I., Watson, A. D., Hama, S., Navab, M., Anantharamaiah, G. M., and Fogelman, A. M. (2008) Anti-inflammatory apoA-I-mimetic peptides bind oxidized lipids with much higher affinity than human apoA-I. *J. Lipid Res.* **49,** 2302–2311
84. Culnan, D. M., Cooney, R. N., Stanley, B., and Lynch, C. J. (2009) Apolipoprotein A-IV, a putative satiety/antiatherogenic factor, rises after gastric bypass. *Obesity* **17,** 46–52
85. O'Looney, P., Irwin, D., Briscoe, P., and Vahouny, G. V. (1985) Lipoprotein composition as a component in the lipoprotein clearance defect in experimental diabetes. *J. Biol. Chem.* **260,** 428–432
86. Kim, S. W., Hwang, H. J., Kim, H. M., Lee, M. C., Shik Lee, M., Choi, J. W., and Yun, J. W. (2006) Effect of fungal polysaccharides on the modulation of plasma proteins in streptozotocin-induced diabetic rats. *Proteomics* **6,** 5291–5302
87. Gianazza, E., Eberini, I., Villa, P., Fratelli, M., Pinna, C., Wait, R., Gemeiner, M., and Miller, I. (2002) Monitoring the effects of drug treatment in rat models of disease by serum protein analysis. *J. Chromatogr. B Analyt. Technol. Biomed. Life Sci.* **771,** 107–130
88. Fujita, T., Suzuki, K., Tada, T., Yoshihara, Y., Hamaoka, R., Uchida, K., Matuo, Y., Sasaki, T., Hanafusa, T., and Taniguchi, N. (1998) Human erythrocyte bisphosphoglycerate mutase: inactivation by glycation in vivo and in vitro. *J. Biochem.* **124,** 1237–1244
89. Sasaki, K., Chancellor, M. B., Goins, W. F., Phelan, M. W., Glorioso, J. C., de Groat, W. C., and Yoshimura, N. (2004) Gene therapy using replication-defective herpes simplex virus vectors expressing nerve growth factor in a rat model of diabetic cystopathy. *Diabetes* **53,** 2723–2730
90. Dahiya, R., Chui, R., Perinchery, G., Nakajima, K., Oh, B. R., and Lue, T. F. (1999) Differential gene expression of growth factors in young and old rat penile tissues is associated with erectile dysfunction. *Int. J. Impot. Res.* **11,** 201–206